J Mater Sci (2007) 42:3044–3054
DOI 10.1007/s10853-006-0535-4

ADVANCES IN GEOPOLYMER SCIENCE & TECHNOLOGY

Physical evolution of Na-geopolymer derived from metakaolin up to 1000 °C

Peter Duxson · Grant C. Lukey · Jannie S. J. van Deventer

Received: 19 October 2005 / Accepted: 6 June 2006 / Published online: 3 February 2007

Abstract The thermal shrinkage and weight loss of a systematic series of geopolymers with nominal composition of $NaAlO_2(SiO_2)_z \cdot 5.5H_2O$ $(1.15 \le z \le 2.15)$ made by activation of metakaolin with sodium silicate solutions are presented. The thermal behaviour of Na-geopolymers are varied, but may be categorised into four regions of behaviour exhibited by all specimens. This investigation explores the effect of nominal Si/Al on the processes and mechanisms of thermal shrinkage and weight loss throughout constant heating of Na-geopolymer. The overall thermal shrinkage of Na-geopolymer increases with increasing nominal Si/Al, with the onset temperature of structural densification occurring at lower temperature with increasing Si/Al. Thermal shrinkage is observed to result from capillary strain, dehydroxylation and viscous sintering in different temperature regions, and is explored by use of dilatometry, thermogravimetry, nitrogen porosimetry and use of different constant heating rates.

Introduction

Geopolymers are chemically hardened monolithic aluminosilicate gels formed by partial dissolution and polycondensation of aluminosilicate materials, such as fly-ash and calcined clays, in aqueous alkaline environments [1, 2]. Geopolymers have been proposed as an alternative to traditional Ordinary Portland Cement (OPC) for use in construction applications, due to their excellent mechanical properties [3], low temperatures required for synthesis and their intrinsic fire resistance [4]. Like zeolites and some aluminosilicate gels, geopolymers are synthesised in aqueous media, albeit much lower water weight fractions, typically less than 35%. Due to their excellent mechanical properties, the bulk of literature is focussed on the effect and application of different raw materials on the compressive strength of geopolymers [5], chemical impurities [6], and the effect of the chemical composition of the alkali activating solutions [7]. Only a relatively small number of investigations have specifically studied the effects of high-temperature on geopolymeric gels [8–13]. Studies of geopolymeric gel have not explored the effect of gel Si/Al, alkali cation, raw material or impurities. Each of these factors play crucial roles in determining the mechanical properties of geopolymers at ambient conditions and should also be expected to affect greatly the properties of geopolymers at elevated temperatures.

The geopolymer structure is formed from tetrahedrally co-ordinated aluminium and silicon atoms bridged with oxygen [14, 15]. The negatively charged aluminium in IV-fold coordination is balanced via association with monovalent cations, typically sodium and potassium, provided by the alkaline activating solution [1]. The resulting inorganic gel is amorphous to electron diffraction [1, 9, 16], and exhibits a single broad hump in ^{29}Si MAS-NMR spectra, similar to aluminosilicate gels [17]. However, transformation of the amorphous gel into zeolite has been observed, where structural reorganisation is rapid due to an open

P. Duxson · G. C. Lukey · J. S. J. van Deventer (✉)
Department of Chemical and Biomolecular Engineering,
The University of Melbourne, Melbourne, Victoria 3010,
Australia
e-mail: jannie@unimelb.edu.au

microstructure [5, 18, 19]. The microstructure of geopolymers has been observed to vary greatly depending on the Si/Al, a result of variation in the density of the aluminosilicate gel. The change in microstructure appears to be very important to the mechanical properties of geopolymers, with strength observed to increase generally with decreasing gel density [18].

Rahier et al. [13] broadly investigated some thermal properties of a geopolymer of non-prescribed composition synthesised from metakaolin and sodium silicate solution (denoted Na-geopolymer), primarily the dehydration and thermal shrinkage. The specimen investigated by Rahier exhibited shrinkage of approximately 6% during dehydration, without significant densification observed at higher temperatures (>600 °C). More recently, the thermal characteristics of Na-geopolymer with a Si/Al of approximately two has been investigated, revealing a similar region of shrinkage associated with dehydration, but also the specimen was observed to densify at approximately 800 °C [8]. The different thermal shrinkage behaviour of these systems suggests that there are differences in the thermal behaviour of Na-geopolymers with differing composition, which is yet to be elucidated by systematic investigation. Furthermore, the dehydration and densification processes occurring in Na-geopolymers have not been determined. The microstructure of Na-geopolymer is known to be highly dependent on Si/Al, which may play a significant role in determining the material's thermal properties and the effect of elevated temperatures on it's physical properties [18].

The current work will focus on the effect of Si/Al on the thermal shrinkage and weight loss characteristics of Na-geopolymer synthesised from metakaolin. The processes of dehydration, dehydroxylation and densification will be systematically investigated in specimens with nominal composition $NaAlO_2(SiO_2)_z \cdot 5.5H_2O$, where $1.15 \le z \le 2.15$. The chemical, physical and structural changes resulting from thermal exposure will be characterised by DTA, TGA, nitrogen porosometry and dilatometry. The thermal behaviour of Na-geopolymers is characterised into four different regions, allowing for the comparison of geopolymeric gels to other synthetic aluminosilicate gel materials.

Experimental procedure

Materials

Metakaolin was purchased from Imerys (UK) under the brand name of Metastar 402. The molar composition of metakaolin determined by X-ray fluorescence (XRF) was $(2.3:1)SiO_2 \cdot Al_2O_3$ with small amounts of a high temperature form of muscovite as an inert impurity. The Brunauer–Emmett–Teller (BET) surface area [20] of the metakaolin, as determined by nitrogen adsorption on a Micromeritics ASAP2000 instrument, is 12.7 m^2/g, and the mean particle size ($d50$) is 1.58 μm.

Alkaline sodium silicate solutions with composition $SiO_2/Na_2O = R$ (0.0, 0.5, 1.0, 1.5 and 2.0) and $H_2O/M_2O = 11$ were prepared by dissolving amorphous silica (Degussa, 99.9%) in appropriate sodium hydroxide solution (Merck, 99.9%) until clear. Solutions were stored for a minimum of 24 h prior to use to allow equilibration.

Geopolymer synthesis

Geopolymer samples were prepared by mechanically mixing stoichiometric amounts of metakaolin and each of the five alkaline silicate solutions to allow $Al_2O_3/M_2O = 1$ to form a homogenous slurry. After 15 min of mechanical mixing the slurry was vibrated for 15 min to remove entrained air before being transferred to polyethylene moulds, which were sealed. Specimens were cured in a laboratory oven at 40 °C and ambient pressure for 24 h before storage at ambient temperatures in sealed vessels for the prescribed period of time before use in experiments. Specimens used in dilatometry experiments were moulded with L/D of 2 (10 mm × 5 mm) and polished so that their ends were flat and parallel to ensure accuracy. This resulted in five specimens with nominal composition $NaAlO_2(SiO_2)_z \cdot 5.5H_2O$ ($1.15 \le z \le 2.15$), and will be referred to as Na1.15, Na1.40, Na1.65, Na1.90 and Na2.15.

Analytical techniques

Simultaneous DTA and TGA measurements were performed on a Perkin–Elmer Diamond DTA/TGA with platinum sample crucibles. Experiments were performed between 25 and 1050 °C at a heating and cooling scan rate of 10 °C min^{-1} with a Nitrogen purge rate of 200 ml min^{-1}. TMA measurements were performed on a Perkin–Elmer Diamond TMA at a constant heating rate of 10 °C min^{-1} unless otherwise indicated and a Nitrogen purge rate of 200 ml min^{-1}.

N_2 adsorption/desorption of powdered specimens were carried out with a Micromeritics Tristar 3000 (Norcross, GA). The air (water) desorption was performed at 100 °C for typically 24 h. Surface areas were calculated with an accuracy of 10%, from the isotherm data using the BET (Brunauer, Emmet

Teller) method [20]. Cumulative pore volumes were determined with the BJH (Barret, Joyner, Halenda) method [21] using the desorption data. The total pore volume V_{p} was derived from the amount of vapour adsorbed at a relative pressure close to unity, by assuming that pores filled subsequently with condensed adsorptive in the normal liquid state. Nominal density of specimens was determined by the Archimedes method in water and air.

Results and discussion

The thermal shrinkage and weight loss of Na-geopolymers with $1.15 \le$ Si/Al ≤ 2.15 are presented in Figs. 1 and 2, respectively. It can be observed that the overall thermal shrinkage of specimens is influenced greatly by the Si/Al. However, all specimens exhibit essentially identical characteristics of weight loss up to 1000 °C (Fig. 2). All specimens exhibit nominal shrinkage up to 100 °C (Fig. 1), while large amounts of weight are lost, presumably from evaporation of free water (Fig. 2), as observed for Na-geopolymers in previous work [8, 13, 22]. A period of rapid thermal shrinkage is observed in all specimens between approximately 100 and 300 °C (Fig. 1).

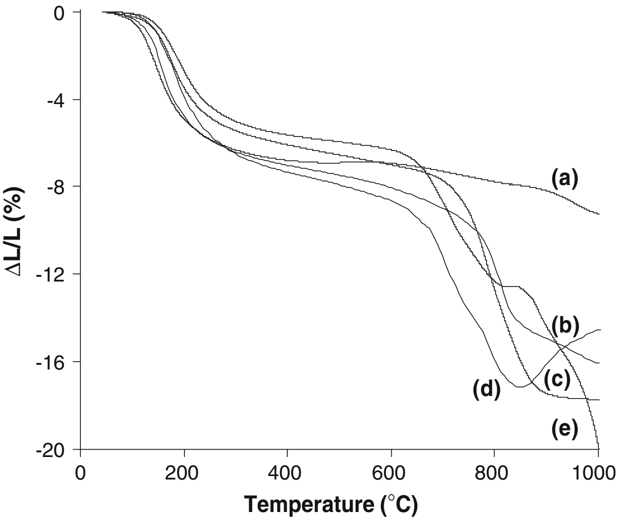

Fig. 1 Thermal shrinkage of Na-geopolymer with Si/Al of: (**a**) 1.15, (**b**) 1.40, (**c**) 1.65, (**d**) 1.90 and (**e**) 2.15

By comparing Figs. 1 and 2, it can be seen that the end of the initial region of rapid shrinkage coincides with a large decrease in the rate of weight loss from dehydration. There is some effect of Si/Al on the onset temperature of the large period of shrinkage observed at approximately 100 °C. The onset temperature of shrinkage for low Si/Al specimens (i.e. Na1.15 and Na1.40) is lower than for specimens with Si/Al ≥ 1.65 (Fig. 1). The slow and constant thermal shrinkage of all specimens appears similar in the temperature region from 300 °C until the onset of rapid shrinkage in the specimens with Si/Al ratio ≥ 1.40 (Fig. 1). The slow rate of thermal shrinkage between approximately 300 and 600 °C may be linked to the slow rate of weight loss observed in the thermogravimetric data (Fig. 2). In contrast to specimens with Si/Al ≥ 1.40, the Na1.15 specimen exhibits only nominal thermal shrinkage beyond 300 °C, with no readily observable region of rapid shrinkage at high temperature despite weight loss that appears similar to all other specimens. However, the Na1.15 specimen does undergo some level of high-temperature thermal shrinkage, suggesting that is may be far more stable at high temperature compared to the higher Si/Al specimens rather than fundamentally different. Nonetheless, from Fig. 1 it can be observed that some characteristic similarities may be observed in the thermal shrinkage of Na-geopolymers with different Si/Al, and also some fundamental differences. Si/Al can be observed to only have a small affect on the weight loss of Na-geopolymers (Fig. 2), yet thermal shrinkage changes significantly at temperatures in excess of 700 °C (Fig. 1). Therefore, differences in

Fig. 2 Percentage weight loss of geopolymer with Si/Al of 1.15, 1.40, 1.65, 1.90 and 2.15. (**a**) Ambient to 1000 °C, (**b**) Ambient to 400 °C

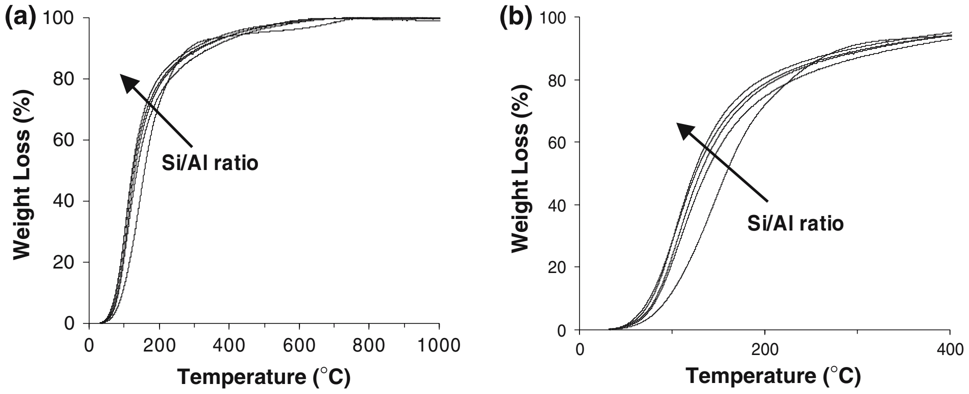

the structure of the material, not specifically related to dehydration are likely to be significant in the determination of geopolymer thermal shrinkage at high temperature.

Small increases in temperature above ambient result in all geopolymer specimens in the current work exhibiting significant weight loss and only nominal shrinkage, which correlates with previous observations [8, 13, 22]. It can be seen from comparison of specimens with different Si/Al in Fig. 1, that there is a compositional dependence of the onset temperature of initial shrinkage and the rate of weight loss. Both the rate of weight loss and the onset temperature of shrinkage decrease with increasing specimen Si/Al. The large fraction of weight loss observed below 300 °C is presumably due to the loss of evaporable water from large pores. As such, the porosity and pore distribution is likely to play a role in determining the rate of dehydration of the specimens in Fig. 2b. Hydrous silicate gels formed by the sol–gel method exhibit gradual shrinkage once exposed to temperatures above ambient, on the order of a few percent by 200 °C in constant heating rate experiments [23]. The shrinkage is accompanied by a much lower fraction of dehydration, and is attributed to the increase in surface area due to desorption of water. Geopolymers are synthesised as monoliths, where water required in synthesis is distributed in the final diphasic structure (i.e. gel and water). Therefore, geopolymers contain a relatively large amount of water available for evaporation in large pores, which would not result in capillary strain. This may account for the low temperature region of dimensional stability, despite the large amount of weight loss routinely observed in dilatometric investigations [8, 13, 22]. Once the freely evaporable water is removed from pores, the gel structure should be subjected to increases in surface area as water is liberated from the surface of the gel and small pores resulting in shrinkage as observed (Fig. 1). The gel contraction in this temperature region may be correlated with the reduction in surface area of specimens discussed later in this article.

It can be observed in Fig. 1 that the temperature of initial shrinkage increases with Si/Al < 1.65. Specimens with Si/Al ≥ 1.65 exhibit similar onset temperatures of shrinkage. A recent study reported that the mechanical properties of Na-geopolymers rapidly improve for 1.15 ≤ Si/Al ≤ 1.65 [18]. It was observed that the Young's modulus of Na-geopolymer increased from approximately 2.3 GPa for Na1.15 to 5.1 GPa for Na1.65 and was similar in specimens with Si/Al ≥ 1.65. The large increase in Young's modulus with increasing Si/Al would provide specimens of higher Si/Al with greater rigidity to resist the capillary strain forces developed during dehydration and may account for the additional dimensional stability of Na-geopolymers with Si/Al ≥ 1.65 in Fig. 1. The increase in the temperature of initial shrinkage observed in Na-geopolymers with 1.15 ≤ Si/Al ≤ 1.65, with similar onset temperatures exhibited by specimens with Si/Al ≥ 1.65 supports this reasoning.

After the initial period of dimensional stability, Na-geopolymers exhibit an onset of rapid shrinkage between approximately 100–300 °C (Fig. 1). The mechanical properties of Na-geopolymers have been observed to vary substantially with Si/Al, which may explain the amount of thermal shrinkage observed in specimens after heating to 300 °C in Fig. 1 [8, 13]. The amount of thermal shrinkage decreases for 1.15 ≤ Si/Al ≤ 1.65, with specimens with Si/Al ≥ 1.65 exhibiting a similar extent of shrinkage. This trend is similar to that observed in the Young's moduli of Na-geopolymers of analogous composition. Similar extent of shrinkage up to 300 °C has previously been observed by Barbosa & MacKenzie [8], who described magnitude of the shrinkage as small, although it accounted for up to one third of all shrinkage observed in their investigations throughout heating to 1000 °C. Rahier et al. [13] attributed shrinkage observed below 300 °C to dehydroxylation. However, dehydroxylation generally occurs at temperatures well in excess of 250 °C. Therefore, evaporation of free pore water is more likely to account for the bulk of weight loss at these lower temperatures. The mechanism responsible for the thermal shrinkage observed up to 300 °C is discussed in more detail later in this article.

Figure 3 shows the DTA thermograms of Na-geopolymer with 1.15 ≤ Si/Al ≤ 2.15. It can be observed that there are two characteristic features of the thermograms; (1) a large endotherm at low temperature (up to

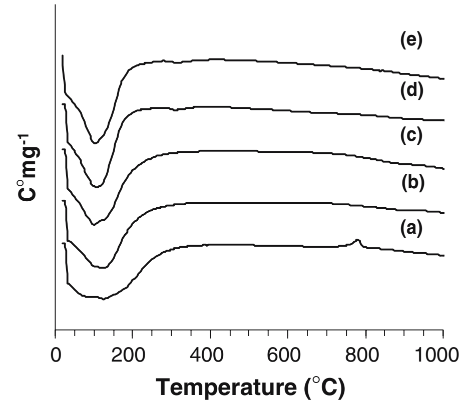

Fig. 3 DTA thermograms of geopolymers with Si/Al ratios of: (**a**) 1.15, (**b**) 1.40, (**c**) 1.65, (**d**) 1.90, and (**e**) 2.15

350 °C) and (2) a period of almost zero gradient. The exothermic peak observed only in the Na1.15 specimen at approximately 700 °C is typical of collapse of zeolitic frameworks. Faujasite has been observed in small amounts in analogous specimens [24], which accounts for this exothermic peak. The endotherm observed in the thermogram of Na1.15 is broad and extends from ambient to 350 °C. As the Si/Al of specimens is increases, the upper bound of the endotherms decrease, and a distinct minimum of greater intensity can be observed to develop at approximately 120 °C (Fig. 3e). The narrowing of the temperature range of dehydration in combination with the appearance of a distinct minimum in the dehydration endotherm with increasing Si/Al implies that a greater proportion of water is evaporated over a more narrow temperature band, which is confirmed by the cumulative weight loss data in Fig. 2.

The increased rate of water loss observed as the Si/Al of specimens increases suggests a change in the structure of the material resulting in different characteristics of dehydration (Fig. 2b). Although it has been observed that the pore size in Na-geopolymers decreases with increasing Si/Al [14, 18], it is apparent that the evaporation of free water in geopolymers is not restricted by pore size. In fact, the greater temperature span of the endotherm in Fig. 3 suggests that Na-geopolymers with low Si/Al (i.e. Na1.15 and Na1.40) contain water that is more tightly bound within the gel. The low Si/Al specimens are known to contain zeolitic 'phase' [24, 25], which tightly incorporate water into their cage-like structure. Therefore, the higher temperature range of dehydration observed in these specimens may be understood. Furthermore, on the order of 80% of all weight loss is observed below a temperature of 300 °C (Fig. 2b), suggesting that the bulk of water in the structure of geopolymeric materials is present as freely evaporable water, with the remainder likely to be present as tightly adsorbed water in small pores or hydroxyl groups on the surface of the gel. Hydroxyl groups are slowly eliminated over a wide temperature region and are therefore unlikely to be observed in DTA thermograms. Therefore, the temperature at which the endotherm observed in the DTA thermogram ends punctuates the end of dehydration.

From a temperature of approximately 300 °C until the onset of rapid shrinkage at approximately 600–750 °C, geopolymers undergo a region characterised by slow concurrent shrinkage (Fig. 1) and weight loss (Fig. 2a). Loss of weight from specimens is observed to last until approximately 750 °C for specimens with Si/Al ≤ 1.40 and approximately 700 °C for specimens with Si/Al ≥ 1.65. Weight loss in this region is characteristic of elimination of water by condensation of silanol or aluminol groups on the surface of the geopolymeric gel, according to the following generalised exothermic reaction:

$$\equiv \mathrm{T}-\mathrm{OH}+\mathrm{HO}-\mathrm{T}\equiv \rightarrow \equiv \mathrm{T}-\mathrm{O}-\mathrm{T}\equiv +\mathrm{H_2O} \qquad (1)$$

where T is Al or Si. The reaction of two hydroxyl groups results in the joining of two surface groups to form part of the aluminosilicate network. Dehydroxylation is therefore limited by several factors including the physical arrangement and dislocation of the hydroxyl groups and their reactivity. The exothermicity of Eq. 1 is determined mainly by the T atoms [26] and to a lesser degree the bond angle of the new linkage [27]. Therefore, the exothermicity of dehydroxylation is ranked (Si + Al) > (Si + Si) > (Al + Al). Similar to the distribution of silicon and aluminium in geopolymer gel [15, 28], the distribution of silanol and aluminol groups on the surface of the gel will be determined by the nominal Si/Al of the specimen. Hence, the energy released from dehydroxylation will increase with decreasing Si/Al, as the proportion of aluminol groups increases. Therefore, the increased temperature span of dehydroxylation of Na-geopolymer as the Si/Al decreases may be understood. Furthermore, the slight thermal shrinkage as observed in Fig. 1 is expected during dehydroxylation from the physical contraction of the gel resulting from the creation of T–O–T linkages. Though the rate of shrinkage and weight loss in this region appear similar in all specimens (Figs. 1 and 2), the duration of shrinkage characteristic of dehydroxylation can clearly be observed to increase with decreasing Si/Al in Fig. 1, confirming that the different ordering of silicon and aluminium in Na-geopolymers is important in determining the thermal properties [14, 15].

Figure 4 shows the BET surface area of Na-geopolymers in the current work, with corresponding pore volume values presented in Fig. 5. Although the pore volume of geopolymers are shown to decrease with increasing Si/Al (Fig. 5), it can be observed that the surface area of the gel accessible to nitrogen does not follow the same simple relation at ambient conditions. Though the pore volume may be predicted from consideration of solution chemistry [18], distribution of pore volume that determines the pore surface area is more complex, and is largely governed by the average pore size. Thus, the appearance of highly porous and accessible zeolite (faujasite) [24] in the Na1.15 specimen accounts for its high BET surface area (Fig. 4). The reduction in pore size that has been observed

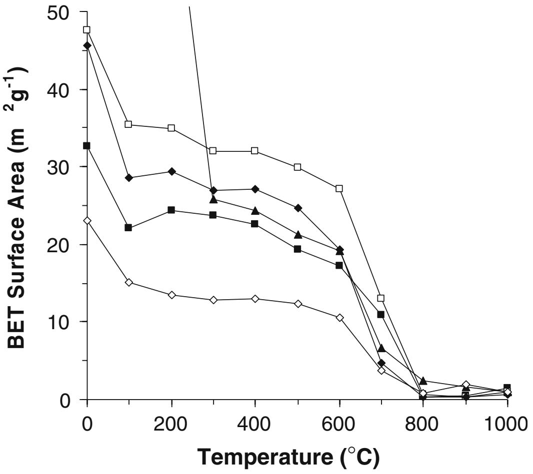

Fig. 4 BET surface area of Na-geopolymer annealed for 2 h between ambient and 1000 °C with Si/Al of (▲) 1.15, (■) 1.40, (□) 1.65, (◆) 1.90, and (◇) 2.15

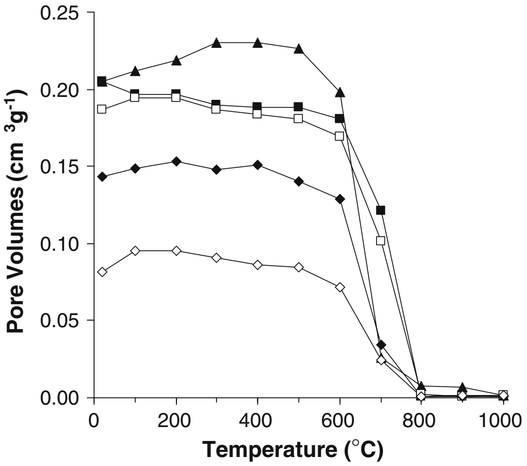

Fig. 5 Pore volume of Na-geopolymer annealed for 2 h between ambient and 1000 °C with Si/Al of (▲) 1.15, (■) 1.40, (□) 1.65, (◆) 1.90, and (◇) 2.15

between Na1.40 and 1.65 [18] is reflected in the increase in BET surface area (Fig. 4). At Si/Al ≥ 1.65 the BET surface area is observed to decrease progressively, which is a result of pore volume (Fig. 5) being incorporated into the gel as pores too small to measure by nitrogen absorption. The reduction of accessible porosity in high Si/Al specimens (Fig. 5) results in the decrease in skeletal density in these specimens [18]. The small increases in the pore volume generally recorded at 100 °C (Fig. 5) imply that mild heating evaporates free pore water, which leads to an increase in the overall pore volume of all specimens. Between ambient and 100 °C a decrease in BET surface area is observed (Fig. 4), suggesting a decrease in gel surface area from capillary strain induced contraction in the pore structure. This would explain the overall thermal contraction in this temperature region. Therefore, the increase of contraction with decrease in Si/Al observed in this region (Fig. 1) is likely to be a result of the higher weight percentage of water in the low Si/Al specimens, given that the nominal composition is based on a constant stoichiometric quantity of water. By 300 °C it is apparent that the faujasite present in Na1.15 has collapsed, due to the greatly reduced surface area. In the temperature region of concurrent shrinkage and weight loss (300–600 °C), the BET surface area of all specimens is observed to decrease at a slow rate, supporting the constant surface area reduction driven by dehydroxylation.

High rates of shrinkage with little or no appreciable weight loss, also known as densification or sintering is observed in Na-geopolymers with Si/Al ≥ 1.40 (Fig. 1). Although the Na1.15 specimen does not undergo densification to the same or similar extent as higher Si/Al specimens, it does exhibit continual shrinkage above 750 °C, where no loss of weight is recorded (Fig. 2) similar to all other specimens. Therefore, some level of densification may be occurring in this specimen, albeit on a much smaller magnitude than higher Si/Al specimens. In contrast to shrinkage resulting from dehydroxylation observed from 300 °C, the onset temperature and extent of densification observed in Na-geopolymer changes greatly with Si/Al, suggesting composition and gel structure play a role in determining the onset temperature of densification.

The derivative of dilatometric data in Fig. 1 provides for a more sensitive determination of the onset and duration of shrinkage events, as presented in Fig. 6. It can be more clearly observed that the onset temperature of the initial region of shrinkage between 100 and 300 °C increases with Si/Al. Also the onset temperature of densification can be observed to increase with decreasing Si/Al from 610 °C for both Na2.15 and 1.90, to 700 °C for Na1.65, 750 °C for Na1.40 and 870 °C for Na1.15. In addition to the onset temperature of densification decreasing with increasing Si/Al, the temperature region spanning densification can be observed to also increase with Si/Al (Fig. 6), as well as the distinct appearance of two partially overlapping peaks of densification in specimens with Si/Al ≥ 1.65. The increased width of the densification region corresponds with the increase in total densification observed with increasing Si/Al (Fig. 1). However, the appearance of two peaks during the densification of geopolymers with Si/Al ≥ 1.65 in Fig. 6 may be the result of either two separate densification events or the supposition of an expansion event, such as crystallisation, onto a broad densifica-

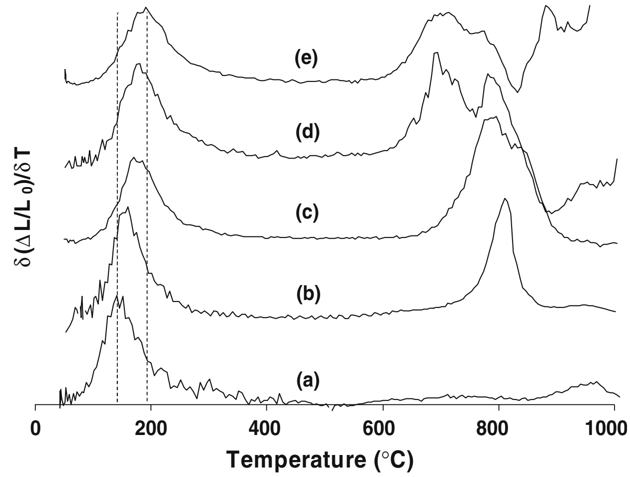

Fig. 6 Differential linear shrinkage measured for Na-geopolymers with Si/Al ratio of (**a**) 1.15, (**b**) 1.40, (**c**) 1.65 and (**d**) 1.90 and (**e**) 2.15. Dotted lines are used to guide the eye

tion event. Before these questions may be understood, the mechanism of densification must be elucidated.

The onset temperature of densification is generally related to the glass transition temperature, T_g, which is one measure of the energy required to break and re-form covalent bonds within the geopolymeric gel [27]. This signifies an increase in mobility of the matrix, i.e. a significant decrease in viscosity resulting in the softening of the material. In sodium alminosilicates where Al/Na is unity, the composition and temperature dependence of viscosity would prescribe that the T_g of Na-geopolymers in the current work should slightly increase with Si/Al, as the strength of Al–O bonds is weaker than Si–O in the presence of sodium [26]. However, it is known that the amount of unreacted material in Na-geoplymers increases with Si/Al [14], which has the effect of reducing the Al/Na ratio in the gel. Therefore, the Al/Na ratio of the gel would be expected to decrease with increase in the Si/Al of the specimen. Al/Na ratios below unity have the effect of lowering the viscosity of aluminosilicates [26], which would explain the decrease in the onset temperature of densification with increasing Si/Al (Fig. 6).

The decrease in densification temperature is not directly observable from surface area (Fig. 4) or pore volume (Fig. 5) measurements on specimens annealed at high temperatures due to their low resolution with respect to temperature. However, large decreases in the surface area and pore volume are observed for all specimens at temperatures >700 °C, corresponding to the onset of densification in Fig. 1. At temperatures >800 °C all specimens exhibit negligible pore volume or surface area, implying that the material has either fully densified, or that the specimens' porosity has become inaccessible. The densification of geopolymer gel may be determined by calculation of the skeletal density. Skeletal density is the density of the gel that is inaccessible to nitrogen in determining adsorption isotherms, and has been shown to decrease with increasing Si/Al of Na-geopolymer [18]. Skeletal density can be evaluated according to the following relation:

$$V_p = \frac{1}{\rho_{\text{nominal}}} - \frac{1}{\rho_{\text{skeleton}}}, \qquad (2)$$

where V_p is the pore volume, ρ_{nominal} is the nominal density and ρ_{skeleton} is the skeletal density. The skeletal density of geopolymeric materials is a measure of the density of the skeletal framework of the gel itself, as opposed to the nominal density of the monolith, which is an averaged density of gel and pores. Since the skeletal density of the gel decreases with increasing Si/Al, the internal surface area of the gel increases, which increases the driving force for densification by providing a large free surface energy [29]. As densification involves reduction in framework surface area, the extent and rate of densification should also be dependent on the physical and chemical structure of the gel. Therefore, the increased duration and extent of densification is also likely to be linked to the skeletal densities of specimens in the current work.

The nominal density of specimens required for the calculation of skeletal density, obtained by annealing of cylindrical specimens for 2 h, are presented in Fig. 7. It can be observed that the nominal density of specimens increase in similar temperature regions and magnitudes corresponding to the linear shrinkage

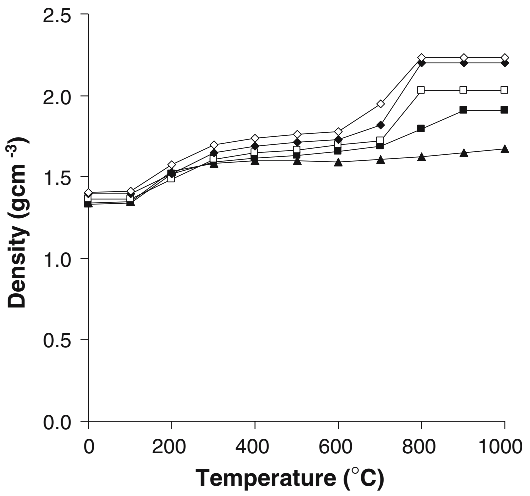

Fig. 7 Nominal density of Na-geopolymer with Si/Al of (▲) 1.15, (■) 1.40, (□) 1.65, (◆) 1.90, and (◇) 2.15

observed in Fig. 1. However, a clear trend in the increasing density of specimens with increasing Si/Al after heating to 1000 °C is also evident, implying that the extent of densification increases with Si/Al, as predicted from consideration of the free energy driving force for skeletal densification.

The calculated skeletal densities from the pore volume (Fig. 5) and nominal densities (Fig. 7) are presented in Fig. 8. It can be observed that the skeletal density of Na-geopolymer increases rapidly in all specimens during the initial region of shrinkage between 100 and 300 °C, corresponding with capillary contraction of the gel in this temperature region. Furthermore, the slight increase of the skeletal density during dehydroxylation between 300 and 600 °C is expected. However, the calculated skeletal densities of Na-geopolymers at temperatures >600 °C appear adversely affected by the pore volume measurements in Fig. 5. In particular the values for specimens with Si/Al ≤ 1.65 are observed to reduce below realistic values, which suggests that the massive reduction in pore volume and surface in Figs. 4 and 5 may be the result of viscous flow and sintering of the gel. Viscous flow is consistent with the mechanism and order of densification observed in Fig. 1, and has been widely observed in silicate gels [27]. Viscous flow would result in porosity being inaccessible to measurement by adsorption. Hence, the skeletal densities calculated in Fig. 8 would appear to be artificially reduced. The skeletal density of specimens with Si/Al ≤ 1.90 exhibit behaviour typically observed during sintering, where the density increases as a result of skeletal densification. However, these values are also likely to be low also, given the negligible pore volume measurements for these specimens at temperatures >800 °C. Therefore, the skeletal density values in Fig. 8 should not be adopted as absolute measures of the skeletal density of the gel. Rather, skeletal density shown in Fig. 8 provides an indication that porosity in geopolymers does not remain accessible after densification. This suggests that the gel may undergo localised viscous sintering, which creates isolated porosity as opposed to a fully densified glass, and would account for the reduction in pore volume to zero in Fig. 5 after the onset temperature of densification.

The densification process of gel is well known to be kinetically limited and that several processes contribute to the overall densification at high temperature [23]. Therefore, the rate of constant heating in dilatometric experiments should have a large effect on the densification process, including the extent of densification. Figure 9 shows the linear shrinkage of Na1.65 for heating rates of 1, 2, 5, 10 and 20 °C min^{-1}. The Na1.65 specimen was chosen as it exhibits a significant degree of densification.

It can be observed that the temperature of initial shrinkage is reduced by reduction in constant heating rate, and the onset temperature of densification appears to be similar despite alteration of heating rate. However, there is no obvious trend linking constant heating rate to the extent of shrinkage observed at 1000 °C, implying that thermal shrinkage of Na-geopolymer is both increased and decreased by changes in constant heating rate at different temperature regions. Figure 10 shows the weight loss of Na1.65 subjected to increasing constant heating rates. It can be observed that slow heating rates result in greater loss of water with respect to temperature. The

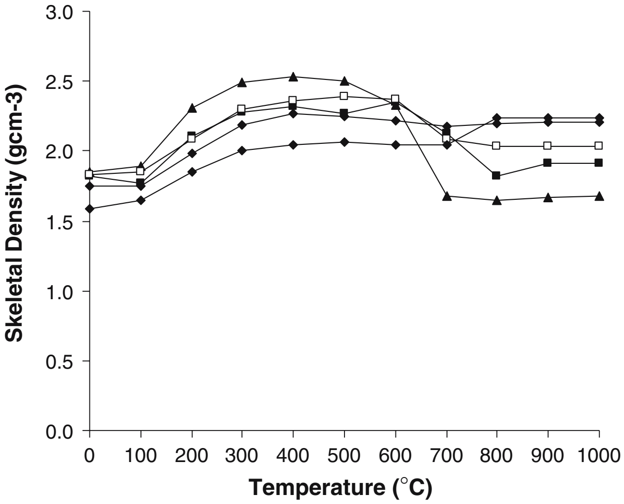

Fig. 8 Skeletal density of Na-geopolymer with Si/Al of (▲) 1.15, (■) 1.40, (□) 1.65, (◆) 1.90, and (◇) 2.15

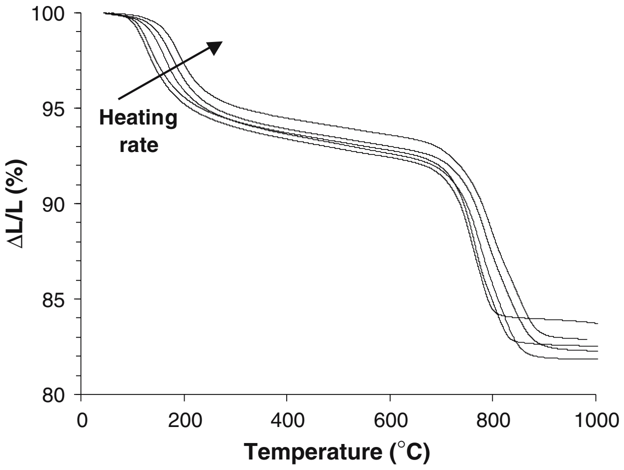

Fig. 9 Linear shrinkage of Na-geopolymer with Si/Al ratio of 1.65 measured at heating rates of 1, 2, 5, 10, and 20 °C min^{-1}. The arrow indicates increasing constant heating rate

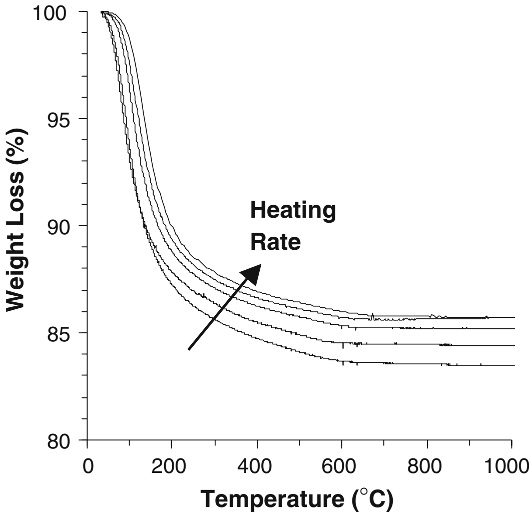

Fig. 10 Weight loss of Na-geopolymer with Si/Al ratio of 1.65 measured at heating rates of 1, 2, 5, 10, and 20. The arrow indicates increasing constant heating rate

different rate of water loss becomes pronounced below 300 °C, with the difference in mass loss at 300 °C approximately maintained through to 1000 °C. As discussed earlier, water loss below 300 °C is predominantly from freely evaporable water. Slow constant heating rates would therefore be expected to result in faster evaporation with respect to temperature on a purely kinetic basis. The similarity of the 1 and 2 °C min^{-1} weight loss curves up to 300 °C implies that weight loss during evaporation is not limited below 2 °C min^{-1}, which is reasonable. The ultimate weight loss of specimens can be observed to increase with decreasing constant heating rate (Fig. 10), suggesting that the rate of weight loss may be influenced by diffusion limited evaporation and kinetics of dehydroxylation from 300 °C until approximately 600 °C, where weight loss is halted. The effect of heating rate on weight loss decreases at the high heating rates, with the weight loss observed in Na1.65 specimens heated at rates of 10 and 20 °C min^{-1} being almost identical. The reduction in the effect of heating rate on weight loss at high rates implies that diffusion is not limiting weight loss, and that the process is limited somehow at higher heating rates, most likely by the physical dislocation of hydroxyl groups during dehydroxylation. The end of weight loss above the densification temperature may be a result of viscous sintering isolating condensed water from escape, and would result in the production of partially hydrous specimens, with implication discussed below.

From Figs. 9 and 10 it is clear that there are four characteristic regions of geopolymer thermal shrinkage; Region I involves loss of freely evaporable water with only nominal shrinkage; Region II is delineated by the onset of initial shrinkage and the continued significant loss of weight; Region III is characterised by gradual loss of both weight and thermal shrinkage and; Region IV involves densification and sintering and is characterised by rapid thermal shrinkage and only nominal weight loss. These characteristics are observed in the thermal shrinkage and weight loss of the other Na-geopolymers in the current work (Fig. 1) and also in previous investigations [8, 13, 22], and appear to be characteristic of all Na-geopolymers.

Figure 11 shows the degree of linear shrinkage observed in the different characteristic regions proposed for Na1.65 subjected to different constant heating rates. Regions I and II are amalgamated for simplicity, and represent shrinkage up to approximately 350 °C, with Region III representing shrinkage between 350 and 700 °C, and Region IV incorporates all shrinkage above 700 °C. As can be observed in Fig. 11, the amount of shrinkage in Regions I and II decreases slightly with increased heating rate as is also observed readily in Fig. 9, and thermal shrinkage in Region III is independent of heating rate. However, thermal shrinkage observed in Region IV during densification increases considerably with increased heating rate. The increased weight loss with respect to temperature of Na1.65 in Regions I and II with decreasing constant heating rate corresponds with increasing shrinkage observed in Fig. 9. The independence of thermal shrinkage in Region III from heating rate implies that shrinkage in this region is not kinetically limited and is a function of temperature alone, which is consistent with dehydroxylation being thermodynamically driven by Si/Al. The increase in the extent of densification with increasing constant heating

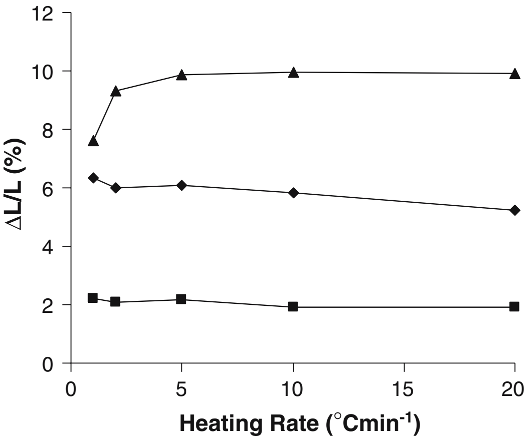

Fig. 11 Linear shrinkage of Na-geopolymer subjected to different heating rates in (◆) Regions I & II (≤350 °C), (■) Region III (350–700 °C) and (▲) Region IV (700–1000 °C)

rate in Region IV suggests that densification may be affected by an increased presence of water in the structure observed in Fig. 10. The amount of water in the structure prior to densification reduces the activation energy for viscous flow [27]. Hence, it is reasonable to suggest that the increase in the extent of densification observed in Fig. 11 may be a result of increased levels of water in the specimen.

Figure 12 introduces the derivative of the dilatometric data for Na1.65 subjected to differing constant heating rates in Fig. 9. It can be observed that the onset temperature of the shrinkage at the beginning of in Region II is unchanged, but that the temperature at the maximum rate of shrinkage is increased by almost 100 °C with increased heating rate. Although the rate of shrinkage with respect to temperature is initially higher for low heating rates, the overall temperature span of Region II is similar for all heating rates. The rate of shrinkage in Region III is identical for all heating rates. The onset temperature of Region IV is not affected by heating rate. However, unlike Region II the temperature range of Region IV is substantially increased, from approximately 150 °C for the heating rate of 1 °C/min up to 300 °C for the heating rate of 20 °C/min. Though the extent of shrinkage observed in Region IV is observed to increase with increasing heating rate (Fig. 11), the increase in temperature span of Region IV with increasing constant heating rate implies that the densification process is kinetically limited to some degree. If the degree of densification is affected by water content, then differences in the viscosity of Na1.65 would be expected throughout Region IV as a function of constant heating rate, and may itself also significantly influence the rate of shrinkage.

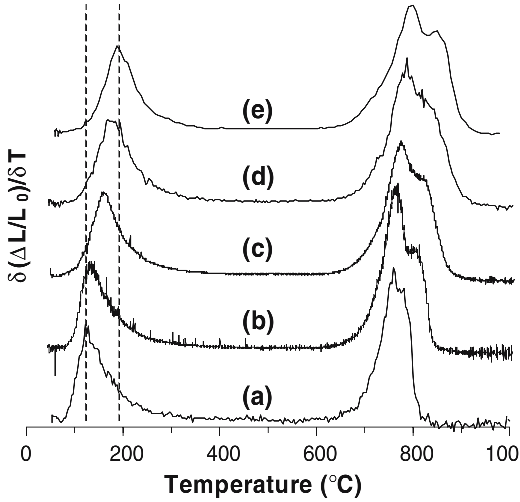

Fig. 12 Differential linear shrinkage of Na-geopolymer with Si/Al ratio of 1.65 measured at constant heating rates of (**a**) 1 °C min^{-1}, (**b**) 2 °C min^{-1}, (**c**) 5 °C min^{-1}, (**d**) 10 °C min^{-1}, and (**e**) 20 °C min^{-1}

Significantly, two distinct regions of shrinkage can be observed in all of the differential shrinkage data in Fig. 12, though the separation of the two shrinkage events increases with the heating rate. The two peaks that appear during the densification of the same specimen occur at increased temperatures as the heating rate increases, suggesting that the second event is dependent on the first, and is not determined by temperature. Therefore, if appearance of two peaks during densification may imply a cascading densification event, or that densification leads to crystallisation. Though no significant crystallisation has been observed in geopolymers synthesised form metakaolin heated in excess of 1000 °C in previous investigations [8], there is evidence to suggest that a more thorough investigation of the possibility of crystallisation of Na-geopolymers should be conducted, particularly given the appearance of a small exotherm consistent with crystallisation in the DTA thermogram of Fig. 3.

Conclusions

The thermal densification and weight loss of Na-geopolymers with 1.15 ≤ Si/Al ratio ≤2.15 have been investigated. In general, the final extent of shrinkage and nominal density observed after heating to 1000 °C increases with Si/Al. Despite large differences in the overall extent of shrinkage and densification temperature, the weight loss observed in Na-geopolymers with different Si/Al are similar, implying that differences in thermal shrinkage are a result of the gel structure. However, the thermal shrinkage and weight loss of all specimens in the current work can categorised into four characteristic regions: Region I involves loss of freely evaporable water with only nominal shrinkage; Region II is delineated by the onset of initial shrinkage and the continued rapid loss of weight; Region III is characterised by gradual loss of both weight and thermal shrinkage and; Region IV involves densification by viscous sintering and is characterised by rapid thermal shrinkage and only nominal weight loss.

The onset temperature of thermal shrinkage at the beginning of Region II was found to relate closely to the published Young's moduli of Na-geopolymers. The mechanism of shrinkage is thought to be capillary shrinkage from evaporation of free water, with the extent of shrinkage in Region II increasing with water content (decreasing Si/Al). The rate of shrinkage in Region III was observed to be similar in all specimens, regardless of Si/Al. However, the temperature span of

Region III was found is related to Si/Al via dehydroxylation. The high temperature required for condensation of aluminol groups is thought to increase the temperature required for complete dehydroxylation in specimens with low Si/Al.

The onset temperature of densification in Region IV decreased with increasing Si/Al, due to incomplete incorporation of aluminium from metakaolin providing free sodium cations, which reduce the T_g of aluminosilicates. Unfortunately, calculation of the skeletal density of geopolymer was observed to be an unreliable method for following the extent of gel densification, but points to the mechanism of densification in Region IV being viscous sintering.

Constant heating rate analysis elucidated that the total fraction of thermal shrinkage of Na-geopolymer up to 1000 °C is not obviously related to heating rate. The extent of thermal shrinkage observed at temperatures in Region II was observed to increase with heating rate, while densification of Na-geopolymer in Region IV increases with increased heating rate. The increase in densification with heating rate is thought to be a result of water being unable to diffuse out of the structure at high heating rates and becoming incorporated into the gel as a hydrous aluminosilicate. Water in the gel lowers the energy barrier to densification and increases the degree of viscous densification observed.

Acknowledgements The authors gratefully acknowledge the financial support of the Particulate Fluids Processing Centre (PFPC), a Special Research Centre of the Australian Research Council (ARC).

References

1. Davidovits J (1991) J Therm Anal 37(8):1633
2. Palomo A, Grutzeck MW, Blanco MT (1999) Cement Concrete Res 29(8):1323
3. Rowles M, O'Connor B (2003) J Mater Chem 13(5):1161
4. Davidovits N, Davidovics M, Davidovits, Ceramic–ceramic composite material and production method. USP 4,888,311, 19 Dec 1989
5. Yip CK, Lukey GC, van Deventer JSJ (2003) Ceramic Trans 153:187
6. van Jaarsveld JGS, van Deventer JSJ (1999) Cement Concrete Res 29(8):1189
7. Phair JW, van Deventer JSJ (2002) Int J Mine Process 66(1–4):121
8. Barbosa VFF, MacKenzie KJD (2003) Mater Res Bull 38(2):319
9. Barbosa VFF, MacKenzie KJD (2003) Mater Lett 57(9–10):1477
10. Cheng TW, Chiu JP (2003) Mine Eng 16(3):205
11. Rahier H, Simons W, Van Mele B, Biesemans M (1997) J Mater Sci 32(9):2237
12. Rahier H, Van Mele B, Biesemans M, Wastiels J, Wu X (1996) J Mater Sci 31(1):71
13. Rahier H, Van Mele B, Wastiels J (1996) J Mater Sci 31(1):80
14. Duxson P, Lukey GC, Separovic F, van Deventer JSJ (2005) Ind Eng Chem Res 44(4):832
15. Duxson P, Provis JL, Lukey GC, van Deventer JSJ, Separovic F (2005) Langmuir 21(7):3028
16. van Jaarsveld JGS, van Deventer JSJ (1999) Indus Eng Chem Res 38(10):3932
17. Aiello R, Crea F, Nastro A, Subotiæ B, Testa F (1991) Zeolites 11(8):767
18. Duxson P, Provis JL, Lukey GC, Mallicoat S, Kriven WM, van Deventer JSJ (2005) Colloid Surf A - Physicochem Eng Aspect 269(1–3):47
19. Palomo A, Blanco-Varela MT, Granizo ML, Puertas F, Vazquez T, Grutzeck MW (1999) Cement Concrete Res 29(7):997
20. Brunauer S, Emmett PH, Teller E (1938) J Am Chem Soc 60:309
21. Barrett EP, Joyner LG, Halenda PP (1951) J Am Chem Soc 73(1):373
22. Barbosa VFF, MacKenzie KJD, Thaumaturgo C (2000) Int J Inorg Mater 2(4):309
23. Brinker CJ, Scherer GW, Roth EP (1985) J Non-Crystal Solids 72(2–3):345
24. Duxson P, Mallicoat S, Lukey GC, Kriven WM, van Deventer JSJ (2005) Ceram Trans 165:71
25. Barrer RM, Mainwaring DE (1972) J Chem Soc - Dalton Trans 22:2534
26. Catlow CRA, George AR, Freeman CM (1996) Chem Commun (11):1311
27. Brinker CJ, Scherer GW (1990) Sol–gel science: the chemistry and physics of sol–gel processing. Academic Press Inc., London, p 980
28. Provis JL, Duxson P, Lukey GC, van Deventer JSJ (2005) Chem Mater 17(11):2976
29. Scherer GW, Brinker CJ, Roth EP (1985) J Non-Crystal Solids 72(2–3):369